SPACECRAFT LEAK LOCATION USING STRUCTUREBORNE NOISE

R. S. Reusser, D. E. Chimenti, S. D. Holland, and R. A. Roberts

Related Articles

Additional information on AIP Conf. Proc.

SPACECRAFT LEAK LOCATION USING STRUCTURE-BORNE NOISE

R. S. Reusser, D. E. Chimenti, S. D. Holland, R. A. Roberts

Center for NDE, Iowa State University, Ames, IA 50014

ABSTRACT. Guided ultrasonic waves, generated by air escaping through a small hole, have been measured with an 8×8 piezoelectric phased-array detector. Rapid location of air leaks in a spacecraft skin, caused by high-speed collisions with small objects, is essential for astronaut survival. Cross correlation of all 64 elements, one pair at a time, on a diced PZT disc combined with synthetic aperture analysis determines the dominant direction of wave propagation. The leak location is triangulated by combining data from two or more detector. To optimize the frequency band selection for the most robust direction finding, noise-field measurements of a plate with integral stiffeners have been performed using laser Doppler velocimetry. We compare optical and acoustic measurements to analyze the influence of the PZT array detector and its mechanical coupling to the plate.

INTRODUCTION

This paper reports on the ongoing development of a phased-array leak location system for manned spacecraft. Based on radar tracking and satellite measurements, there is a very broad spectrum of debris in Earth orbit which has the potential to impact manned spacecraft at very high velocities, causing leakage of the spacecraft atmosphere into the vacuum of space. Roughly a million of those particles are large enough to breach the spacecraft pressure vessel, but are not large enough to track and avoid [2]. Since the weight requirements of shielding are prohibitive for debris on the order of 1 cm or larger [1], a system for rapid location of leaks is necessary. The leak noise itself is generated on the downstream side of a turbulent jet into a vacuum. Since the noise is unable to pass upstream through the Mach 1 jet, detection through the air relies on noise that has first been coupled into the plate, then re-radiated into the spacecraft atmosphere. Instead of relying on this secondary noise, the method investigated here detects noise transmitted directly through the spacecraft skin.

Past work [5] has focused on the development of a detector capable of sensing the dispersive Lamb modes coupled into a plate at the source of a leak. Successful leak location has been shown on a simulated spacecraft structure using an 8×8 diced PZT array detector. By determining the dominant direction of wave propagation with Fourier-based analysis, data from multiple independent sensors triangulates the leak. In an environment where prompt and accurate leak location is critical, the procedure must be robust, so current work focuses on the study of noise propagation in spacecraft structures and the development of a robust algorithm for frequency selection.

One of the main factors determining leak location capability is the geometry of the spacecraft structure. To add additional rigidity with minimal weight, spacecraft structures typically include integrally machined stiffeners of various geometries. These ribs scatter the leak noise and, based on calculations by Roberts using the Boundary Element Method (BEM), act as a filter [6], producing frequency bands with very high transmission across stiffeners, and frequency bands with very low transmission. Despite this complication, the system described has been shown to work in integrally stiffened plates [4], although interaction of the integral stiffeners with the noise field could not be experimentally investigated in tandem with the mechanical and electronic response of the array detector. The current work investigates transmission of noise through a simulated spacecraft structure while idealizing the other components of the system. This establishes an upper bound for performance of the fully integrated system, and provides the necessary guidance for the determination of a robust leak-location algorithm.

ARRAY LEAK LOCATION

The leak location algorithm has been explained previously [5] so only a brief summary is presented here. The signal generated by the leak and arriving at an element of the array can be expressed, for distance $|\vec{x}| \gg 1/k_n(\omega)$, as

$$V(\vec{x},\omega) = N(\omega)|\vec{x}|^{-1/2} \sum_n A_n(\omega) \exp(i\,k_n(\omega)|\vec{x}|), \tag{1}$$

where V represents a voltage at position $\vec{x}$ and frequency ω. N represents the complex amplitude and phase of the noise source, and the traveling waves are summed over all guided wave modes n with amplitude coefficient A_n. Representing the array element position $\vec{x}$ as the sum of a leak-relative array reference position $\vec{x}_0$ and an array-relative element position $\vec{s}$,

$$\vec{x} = \vec{x}_0 + \vec{s}. \tag{2}$$

As illustrated in Figure (1a), the distance to a specific element can be written through a far-field approximation as

$$|\vec{x}| = |\vec{x}_0| + \vec{d} \cdot \vec{s}, \tag{3}$$
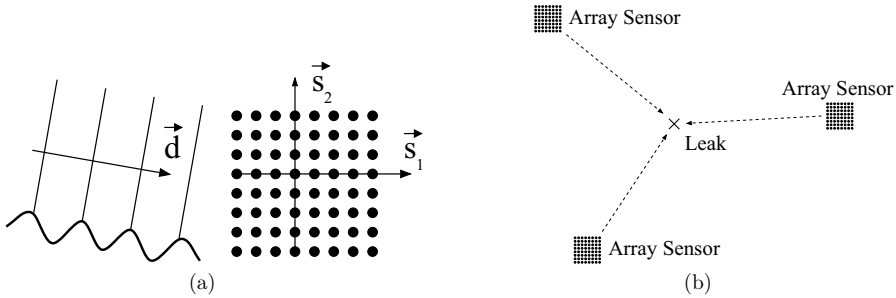
FIGURE 1. (a) Measurement positions in array sensor. (b) Distributed sensors for leak location.

where $\vec{d}$ is a unit vector pointing from the leak to the fixed reference position. Then substitution into Equation (1) yields

$$V(\vec{s}, \omega) = N(\omega)|\vec{x}_0|^{-1/2} \sum_n A_n(\omega) \exp\left[i\, k_n(\omega)(|\vec{x}_0| + \vec{d} \cdot \vec{s})\right]. \tag{4}$$

In the proposed method, the noise source is random-phase so at least two PZT elements must be cross-correlated to create a deterministic signal and locate the leak. However, this work substitutes a scanned laser vibrometer for the PZT array detector, and an impulsive point contact transducer for the air leak, making the cross-correlation unnecessary. The finite size of the array applies a spatial window, $W(\vec{s})$, to the acquired data, then the two-dimensional Fourier Transform of Equation (4) in s_x and s_y gives

$$\text{FT}\left\{W(\vec{s})V(\vec{s}, \omega)\right\} = \sum_n B_n\, \hat{W}(\vec{k} - \vec{k}_n(\omega)\vec{d}), \tag{5}$$

where the amplitude coefficients have been grouped into B_n. Representing the data in a two-dimensional wavenumber map, the energy in all modes n and at frequency ω lies along a line emanating from the origin and in the dominant direction of wave propagation, $\vec{d}$. This direction is easily determined by inspection of the map. As illustrated in Figure (1b), triangulation from multiple independent sensors locates the leak.

FREQUENCY SELECTION

Selection of the proper frequency band is critical to determining the most probable leak location and minimizing the number of required sensors. Three factors determine this frequency band: leak noise spectrum, array detector sensitivity, and noise transmission across structural features. A robust leak location system must operate in the intersection of these three criteria.

Basic turbulence theory predicts the leak energy coupled into the plate will decrease with frequency, and in fact it is observed that no usable leak noise exceeds roughly 400 kHz. This matches the sensitivity of the detector, which operates below 500 kHz. Dicing the PZT array has previously been shown to improve leak location performance [4], but probable reflections and overall poor performance are still observed from 75-275 kHz. The additional complication of integral stiffeners makes it unclear whether the poor performance at certain frequencies is a result of the detector, or whether the integral stiffeners filter the noise. Figure (2) shows stiffener transmission coefficients for a 3/16 inch square stiffener [3]. This suggests that the performance may be a function of stiffener transmission. By idealizing the array detector, there is no ambiguity.

Two different candidate algorithms are considered. The first, termed *in situ* calibration, relies on simulated leaks with a known position. Determination of frequency bands that correctly locate the known leak easily optimizes the system. The most straightforward implementation pairs a contact source transducer with each detector array. Location of one simulated leak at a time with each of the other sensors determines the calibration. Unfortunately, this requires the additional complexity, power, and cost of additional transducers. The second method, termed wide-bandwidth analysis, simply uses the full functional range of the array detector. By integrating over all
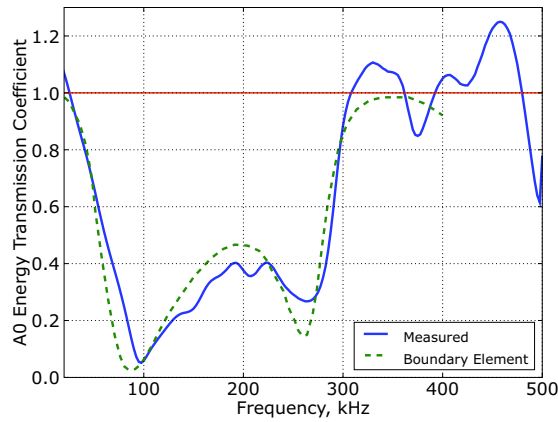
FIGURE 2. Comparison of measured and calculated energy transmission coefficients for low aspect-ratio stiffener.

frequencies which may provide a correct answer, the frequency-dependent reflections tend to cancel destructively, while the correct signals reinforce.

EXPERIMENTAL SETUP

The test section, pictured in Figure (3), is a 6 ft × 6 ft aluminum plate, 3/16 inches thick with 3/16 inch wide × 3/16 inch tall integrally machined stiffeners spaced 1 ft apart on a square grid. Previous tests on this specimen with low aspect-ratio stiffeners have demonstrated consistent leak-location capability across at least five stiffeners with very little degradation in signal quality [4]. It is important to note that although the structure is representative of integrally stiffened spacecraft structures, it is only one of many possibilities.

The current work replaces the PZT array detector with a scanned Polytec laser vibrometer. The vibrometer measures normal velocity of the plate, and a two-axis motion control stage scans the laser across an 8 × 8 array with 2 mm spacing, the same geometry as the PZT array detector. The scanned array remains at the same location for all tests. Unlike the PZT array detector, the vibrometer is an ideal point detector which effectively eliminates coupling inconsistencies and makes any measured characteristics a result of the test section itself.

The leak in these tests is simulated by a point contact transducer. This is achieved with an ultrasonic horn that reduces the contact area down to roughly 1mm². It is verified that the leak noise and the impulsive point source generate almost exclusively the A_0 mode below 400 kHz. This matches the range of the measured spectrum of the leak noise. While the actual spectrum of the transducer does not match that of the leak, linearity of the problem means analysis at narrow frequency bands is indistinguishable from a true leak source. Despite the reduced sensitivity of the laser

264
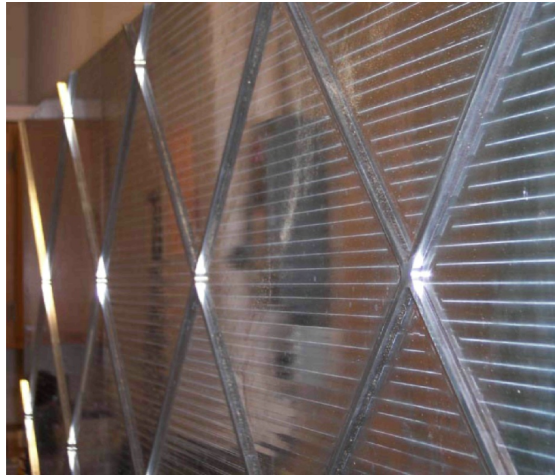
FIGURE 3. 6 ft × 6 ft aluminum plate with 3/16 inch square integrally machined stiffeners.

vibrometer relative to the PZT array detector, the simulated leaks make a much larger number of trials possible.

Forty-three different leak locations are arbitrarily chosen across the surface of the plate, with data for each scan collected over a period of twenty minutes. This is significantly longer than roughly the one minute required for the PZT array, but produces an idealized version of the same measurement. The direction of wave propagation is determined with Equation (5).

RESULTS

The results of these tests for two different frequency ranges are plotted in Figure (4). Each 'x' corresponds to a simulated leak location, and the single circle shows the location of the scanned laser vibrometer. The dashed lines represent the integral stiffeners, and the arrows show the dominant direction of wave propagation as measured at the array. Figure (4a) shows the results of all 43 tests with the wavenumber map integrated over frequencies from 75-100 kHz, while Figure (4b) shows the same tests integrated from 375-400 kHz. For each test, only the strongest wavenumber has been sampled and plotted.

Although some of the simulated leaks are correctly located by the vibrometer, the performance is very poor at 75-100 kHz. Conversely, none of the measurements across as many as four stiffeners are in error at 375-400 kHz by more than 5°. Since there are no complicating effects from the PZT array detector, this behavior is caused entirely by the response of the integrally stiffened plate. This matches very closely the performance of the PZT array detector, which is seen to perform well only above approximately 275 kHz. Furthermore, this also matches the stiffener transmission coefficients of Figure (2) remarkably well. The vibrometer locates the leak with consistent

265
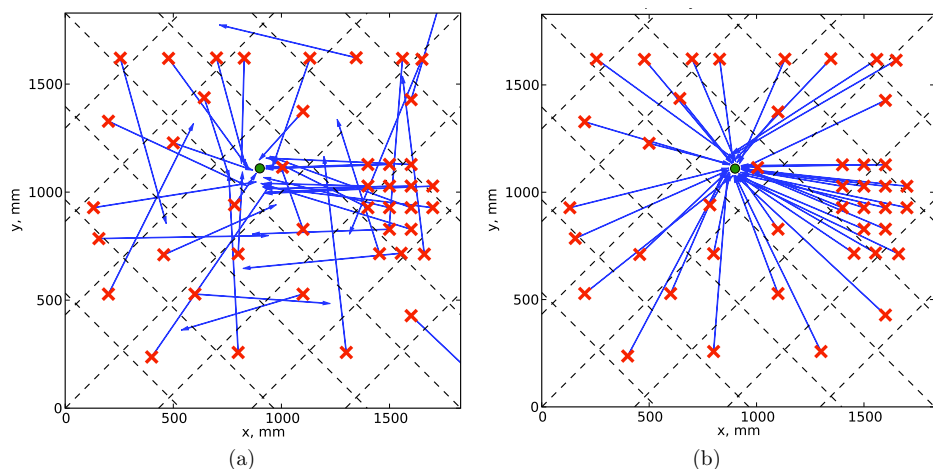
FIGURE 4. Leak location results for frequencies from (a) 75-100 kHz and (b) 375-400 kHz.

accuracy only above 275 kHz. The tests in Figure (4) are not precisely described by normal incidence of the waves upon the stiffener, but the results strongly suggest that normal transmission is a good indicator of leak location performance.

The strong correlation suggests that *in situ* calibration may be the preferable algorithm for frequency selection since it is very clear after examination which frequencies should be utilized. However, not all stiffener geometries have such wide passbands and stopbands. Figure (5) shows measured and calculated transmission coefficients for a high aspect-ratio stiffener measuring 0.8 inches tall × 0.1 inches wide. Again, there are clear passbands and stopbands, but when this data for normal incidence of waves upon a stiffener is perturbed for off-normal incidence across multiple stiffeners, it is no longer as clear which frequencies should be examined.

Figure (6) shows the same data from Figure (4) with the maps normalized and integrated from 100-475 kHz. Normalization prevents a single spurious frequency from dominating the entire result. This wide-bandwidth algorithm demonstrates accurate leak location for 40/43 tests. Although this does not quite match the performance of Figure (4b), it shows that a more robust strategy can still locate leaks with high accuracy.

SUMMARY AND CONCLUSIONS

Optical measurements equivalent to the leak location algorithm have been performed. The results match very closely the performance of the PZT array detector, and provide physical insight into the performance of the full leak location algorithm. Two algorithms for robust frequency selection have been considered. Although the transmission coefficients for waves at normal incidence to a stiffener are not an exact physical model for general leak location, they are demonstrated to provide guidance

266
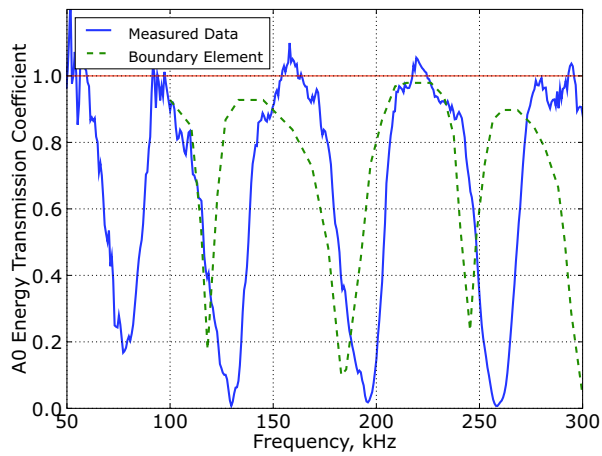
FIGURE 5. Comparison of measured and calculated energy transmission coefficients for high aspect-ratio 0.8 inch tall × 0.1 inch wide stiffener.
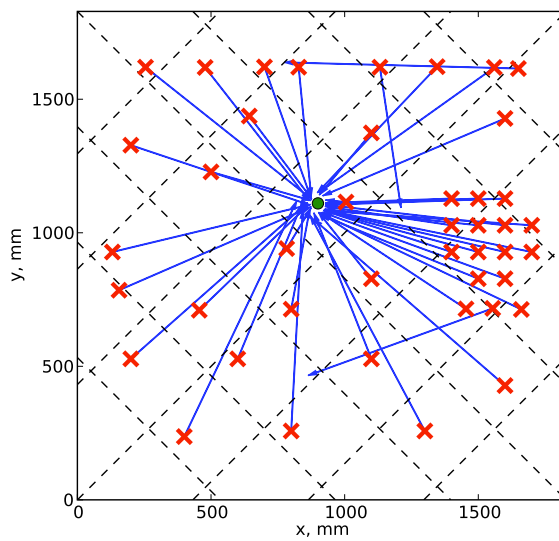
FIGURE 6. Leak location results for combined frequencies from 100-475 kHz.

267

for robust frequency selection. It is determined that although *in situ* calibration works very well under certain conditions, ultimately a robust frequency selection algorithm must be a wide-bandwidth algorithm. Together with the noise spectrum of the leak and the response of PZT array detector, this provides the necessary guidance for frequency selection. Ultimately, there is some room for compromise between the two algorithms. The widest possible bandwidth should be chosen, subject to stiffener transmission and detector sensitivity.

ACKNOWLEDGEMENT

REFERENCES

1. D. J. Kessler. Sources of orbital debris and the projected environment for future spacecraft. *Journal of Spacecraft*, 18(4):357360, 1981.

2. D. S. F. Portree and J. P. Loftus Jr. Orbital debris: A chronology. *NASA Technical Paper*, TP-1999-208856, 1999.

3. R. S. Reusser, D. E. Chimenti, S. D. Holland, and R. A. Roberts. Plate wave transmission/reflection at geometric obstructions: Experiment. *These proceedings.*

4. R. S. Reusser, S. D. Holland, D. E. Chimenti, R. A. Roberts, and S. Sulhof. Leak location in spacecraft skin with ultrasonic arrays. *Review of Progress in Quantitative NDE Vol. 26*, D. O. Thompson, D. E. Chimenti, Eds., 2007.

5. R. S. Reusser, S. D. Holland, R. A. Roberts, and D. E. Chimenti. Array-based acoustic leak location in spacecraft structures. *Review of Progress in Quantitative NDE Vol. 25*, D. O. Thompson, D. E. Chimenti, Eds., 2007.

6. R. A Roberts. Plate wave transmission/reflection at integral stieners. *Review of Progress in Quantitative NDE Vol. 25*, pages 95102, D. O. Thompson and D. E. Chimenti, Eds., 2007.